

8th Red LHC Workshop
Madrid
May 28-30, 2024



Measurement of differential cross sections in $t\bar{t}$ and $t\bar{t}+\text{jets}$ production in the $\ell+\text{jets}$ decay mode in pp collisions at $\sqrt{s} = 13 \text{ TeV}$ using 140 fb^{-1} of ATLAS data

Claudia Glasman
Universidad Autónoma de Madrid



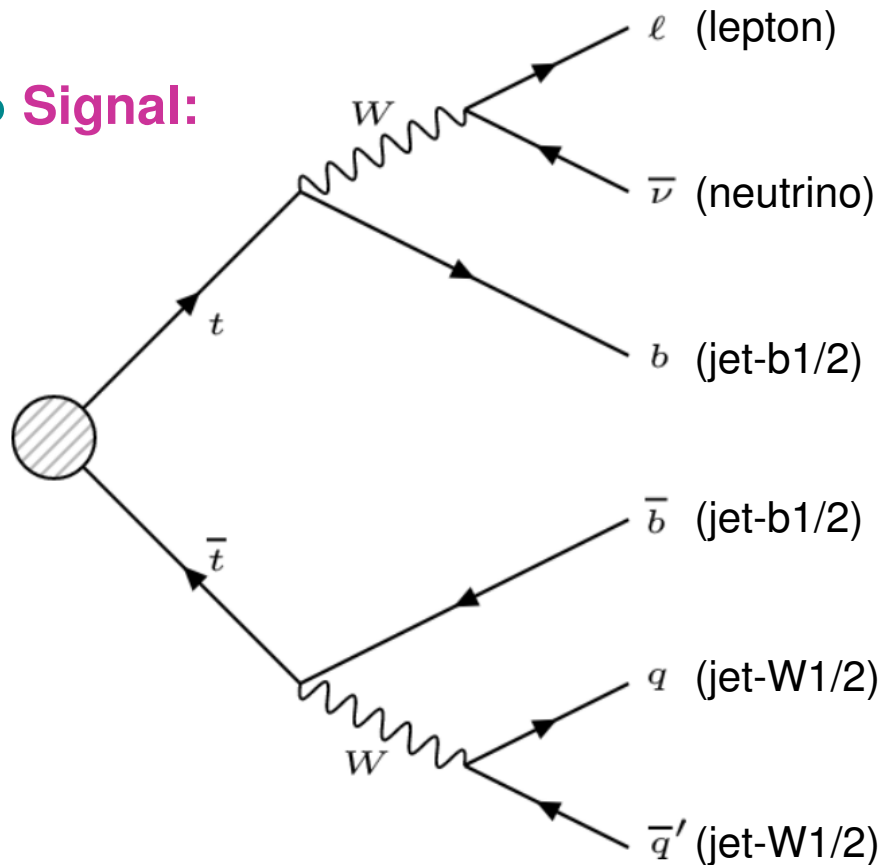
$t\bar{t}$ differential cross sections in the ℓ +jets decay mode



- **Measurements of $t\bar{t}$ and $t\bar{t}$ +jets differential cross sections**
 - pp collisions at $\sqrt{s} = 13$ TeV using 140 fb^{-1}
 - absolute and normalised cross sections at particle level in ℓ +jets decay mode
 - jet observables in three channels: $t\bar{t}$ inclusive, $t\bar{t} + 1\text{jet}$ and $t\bar{t} + 2\text{jets}$
- **Motivation:**
 - characterisation of the kinematics and topology of the $t\bar{t}$ system ($t\bar{t}$ inclusive channel) via transverse momentum and rapidity of jets and their angular correlations
 - characterisation of the kinematics, dynamics and topology of the hardest ($t\bar{t} + 1\text{jet}$ channel) and second-hardest ($t\bar{t} + 2\text{jets}$ channel) QCD emissions via transverse momentum and rapidity of jets and their angular correlations and invariant masses
 - tests of pQCD theory via NLO and NNLO predictions

$t\bar{t}$ signal and background

- **Signal:**



highest (second-highest) p_T additional jet arising from hard QCD radiation: 'jet-rad1/2'

- **Signature for ℓ +jets $t\bar{t}$ processes:**

- charged lepton
- neutrino
- two bottom quarks
- two jets with invariant mass closest to m_W

- **Signature for the $t\bar{t} + 1$ jet channel:**

- at least one additional jet

- **Signature for the $t\bar{t} + 2$ jets channel:**

- at least two additional jets

- **Additional jets can arise from ISR and/or FSR**

- **Background (simulated using MC samples): $\approx 10\%$ in each channel**

- single top (dominant), W +jets, Z +jets, $t\bar{t}V$, diboson and $t\bar{t}H$ (using MC)
- multijets (data-driven method)

Fiducial phase space and QCD predictions



Fiducial phase space (particle level)

- exactly one lepton (e or μ) with $p_T > 27$ GeV and $|\eta| < 2.5$
- at least 4 jets (2 ghost-matched with a B -hadron) with $p_T > 25$ GeV and $|y| < 2.5$
- overlap removal: if $\Delta R(\ell, \text{jet}) < 0.4$, ℓ is removed

● QCD predictions:

- **NLO**: PWG+PY8, PWG+HW7, aMC@NLO+HW7 and SHERPA 2.2.12 (using NNPDF3.0(N)NLO)
- **NNLO (in $t\bar{t}$ system)**: PWG+PY8 MiNNLOPS (using NNPDF3.0NNLO)
- **Normalisation from Top++2.0 at NNLO+NNLL with $m_t = 172.5$ GeV**:

$$\sigma_{t\bar{t}} = 832_{-29}^{+20} \text{ (scale)} \pm 35 \text{ (PDF, } \alpha_s) \pm 23 \text{ (} m_t) \text{ pb}$$
- **Theoretical uncertainties in differential cross sections: scales, PDFs and α_s**
 - **scale variations dominant**: $\approx 10\%$ ($\approx 40\%$) at low (high) p_T at NLO
 $\approx 5\%$ ($\approx 10\%$) at low (high) p_T at NNLO
 - further reduction for normalised cross sections ($\approx 2\%$ at low p_T)

Systematic uncertainties

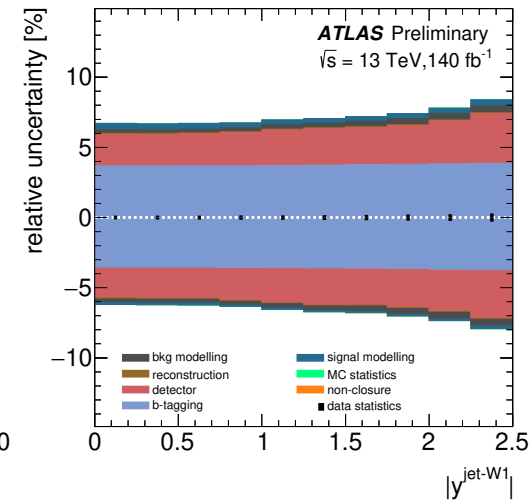
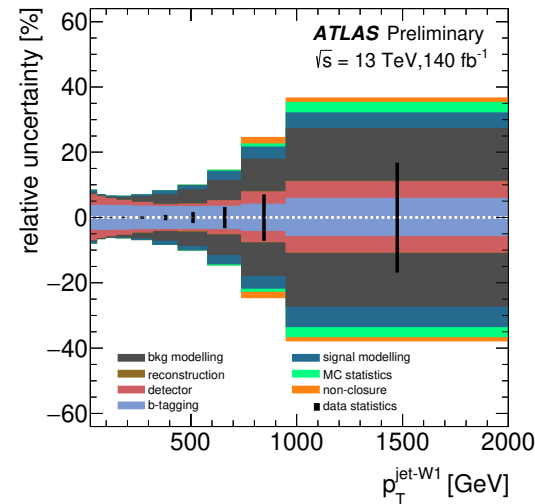
- The following sources of systematic uncertainties were considered:

- b -tagging calibration and efficiency
- detector energy scale and resolution
- reconstruction efficiency
- background modelling
- signal modelling
- non-closure
- statistics
- (luminosity → $\pm 0.83\%$)

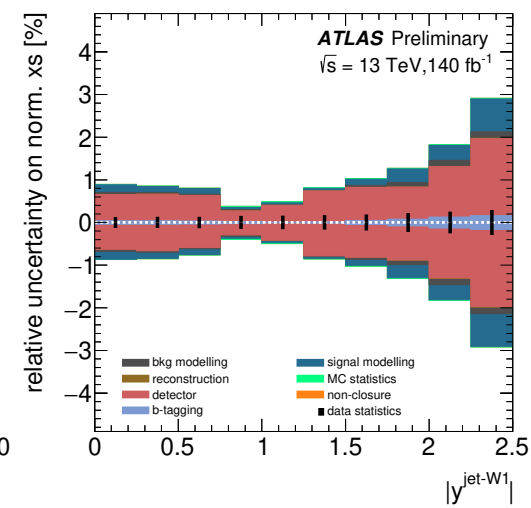
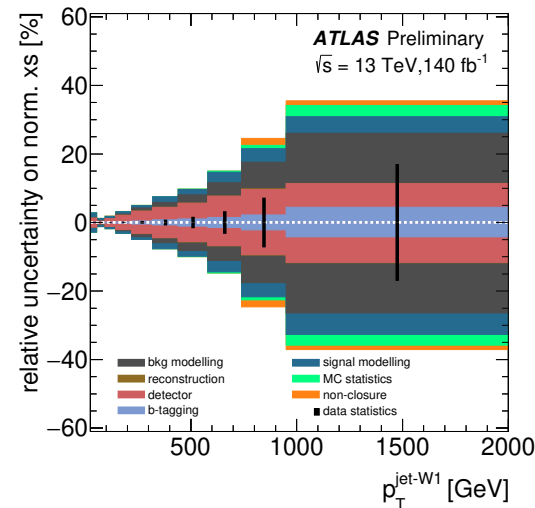
- Total relative uncertainty:

- $\approx 7\%$ ($\approx 1\%$), $\approx 10\%$ ($\approx 1.5\%$) and $\approx 13\%$ ($\approx 2\%$) for $t\bar{t}$ inclusive, $t\bar{t} + 1\text{jet}$ and $t\bar{t} + 2\text{jets}$ at low p_T for absolute (normalised) cross sections

absolute cross sections

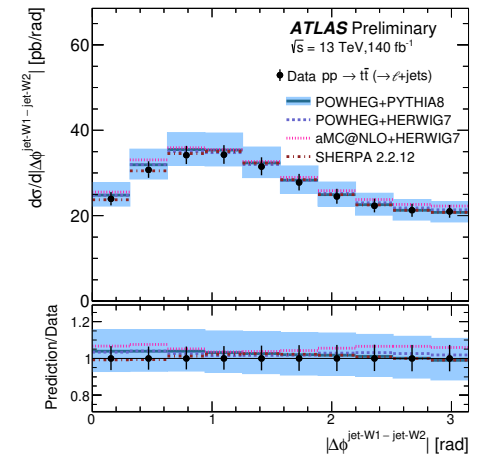
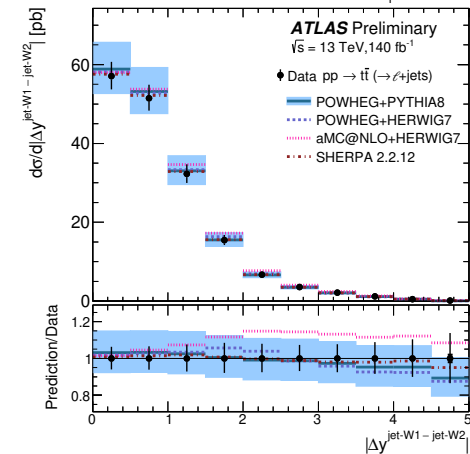
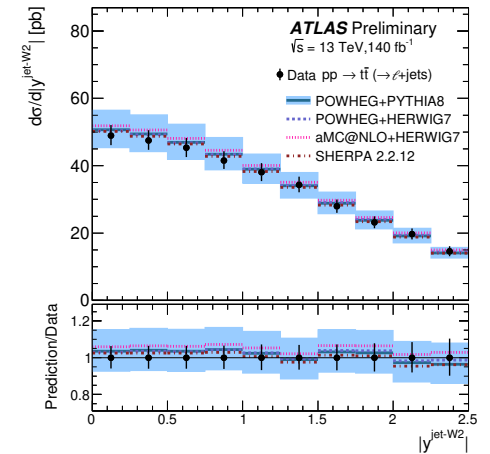
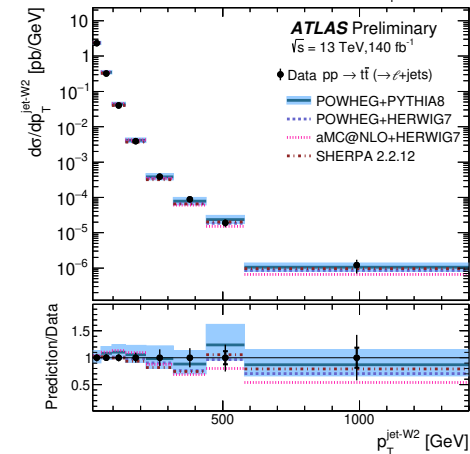
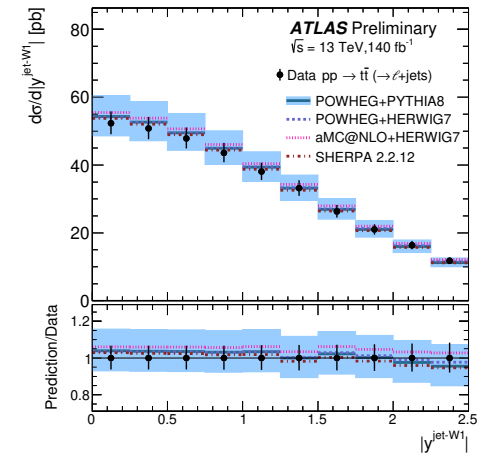
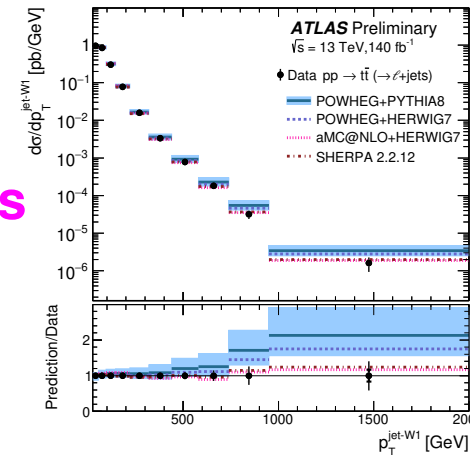


normalised cross sections



Results

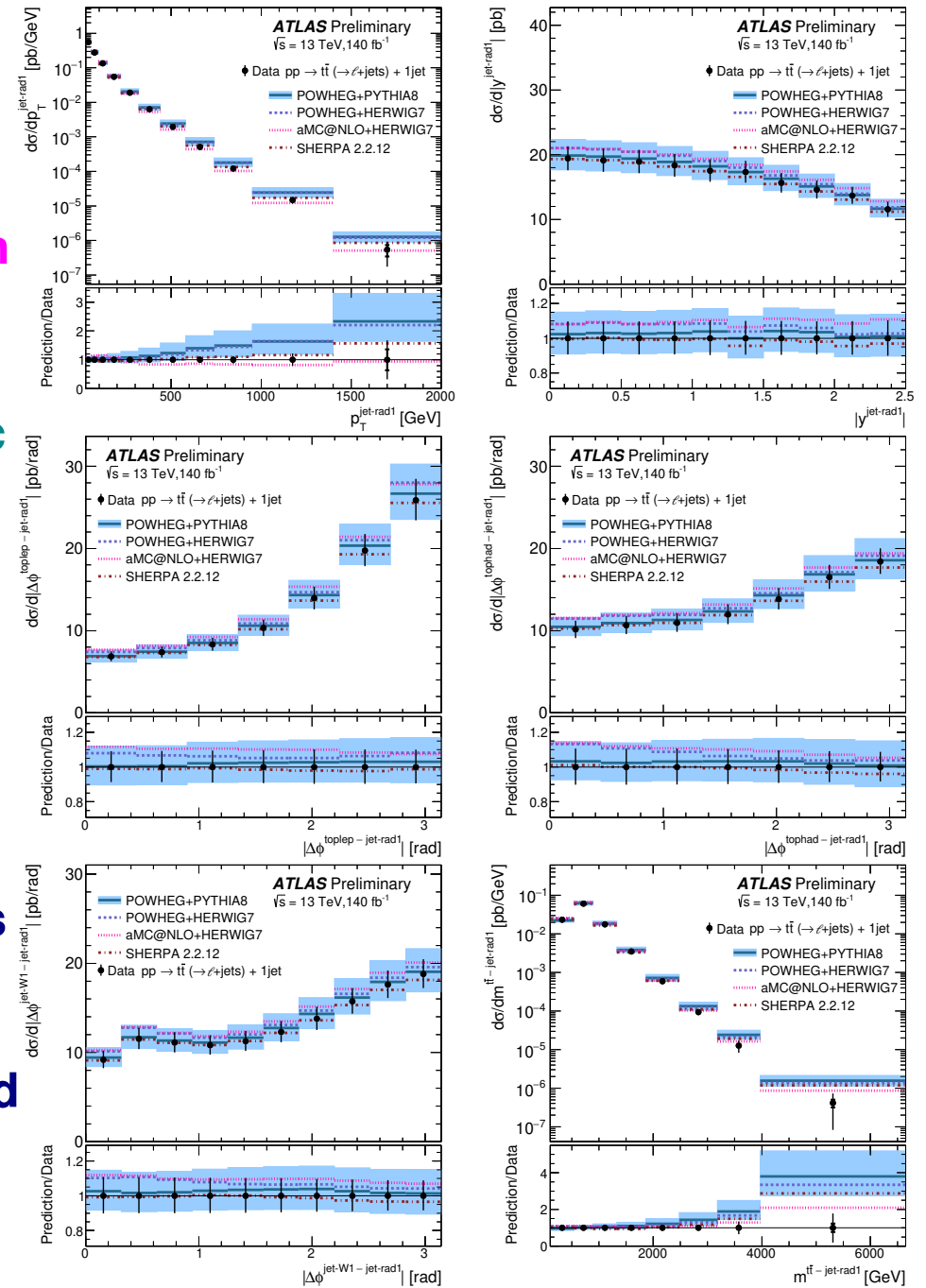
- **Absolute differential cross sections for $t\bar{t}$ inclusive channel vs NLO:**
- **Motivation:** characterisation of kinematics and topology of $t\bar{t}$ system
- **Measured cross section as a function of $p_T^{\text{jet-W1}}$ has a harder spectrum than that of $p_T^{\text{jet-W2}}$**
- **Measured cross sections as functions of $|y^{\text{jet-W1}}|$ and $|y^{\text{jet-W2}}|$ have very similar shape and normalisation**
- **Comparison with NLO QCD predictions:**
 - good description of angular observables
 - good description of $p_T^{\text{jet-W1}}$ by SHERPA and aMC@NLO+Hw7
 - $p_T^{\text{jet-W2}}$ is in general well described



Results

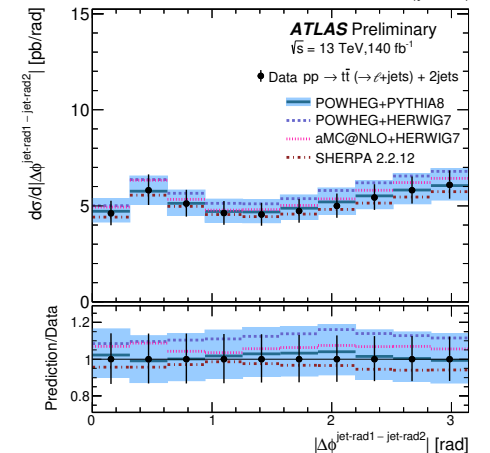
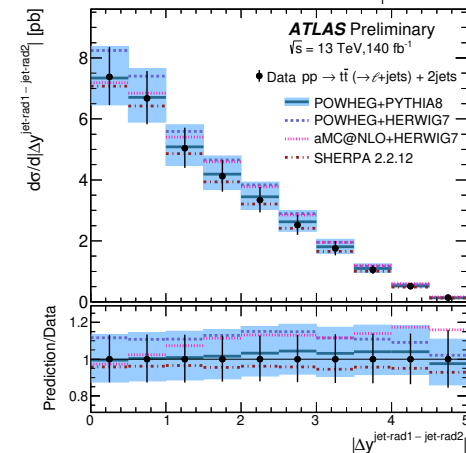
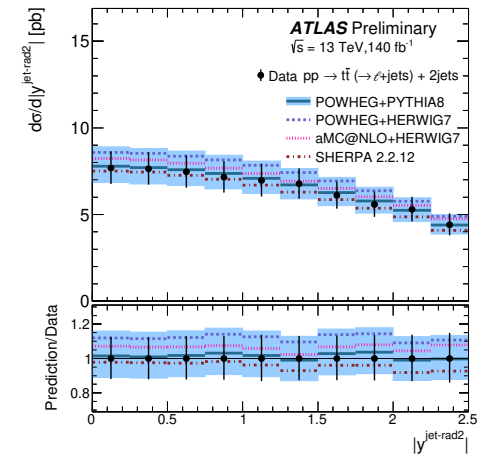
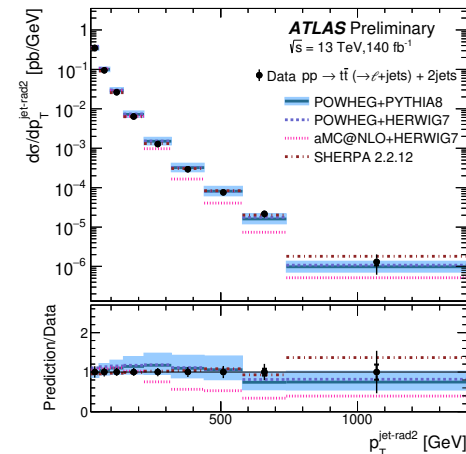
- **Absolute differential cross sections for $t\bar{t}+1$ jet channel vs NLO:**
- **Motivation:** characterisation of kinematics, dynamics and topology of hardest emission
- **Measured cross section as a function of $|y^{\text{jet-rad1}}|$ is different than that of $|y^{\text{jet-W1}}|$**
 → first emission tends to be more isotropic than the jets forming the tophad
- **Measured cross sections as functions of $|\Delta\phi^{\text{toplep-jet-rad1}}|$ and $|\Delta\phi^{\text{tophad-jet-rad1}}|$ have different shapes**
 → the hard radiation tends to be farther in ϕ from the toplep than from the tophad
- **Comparison with NLO QCD predictions:**
 - good description of angular observables
 - good description of $p_T^{\text{jet-rad1}}$ by SHERPA and aMC@NLO+Hw7
 - $m^{\text{t}\bar{t}-\text{jet-rad1}}$ is in general well described by aMC@NLO+Hw7

ATLAS Collab, ATLAS-CONF-2023-068



Results

- Absolute differential cross sections for $t\bar{t}+2$ jets channel vs NLO:
- **Motivation:** characterisation of kinematics, dynamics and topology of second hardest emission
- Measured cross section as a function of $|y^{\text{jet-rad2}}|$ is different than that of $|y^{\text{jet-W1}}|$
 → second emission tends to be more isotropic than the jets forming top had
- $|\Delta y^{\text{jet-rad1} - \text{jet-rad2}}|$ has different shape than $|\Delta y^{\text{jet-W1} - \text{jet-W2}}|$
- $|\Delta\phi^{\text{jet-rad1} - \text{jet-rad2}}|$ has different shape than $|\Delta\phi^{\text{jet-W1} - \text{jet-W2}}|$

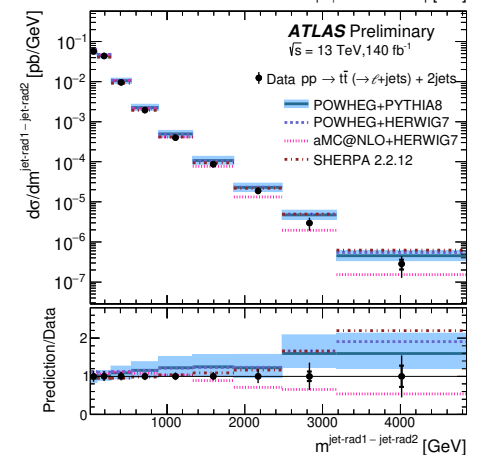
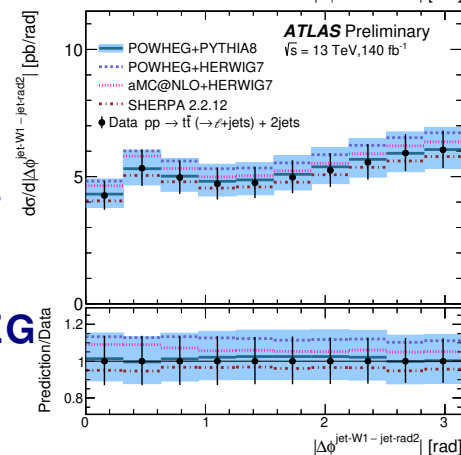
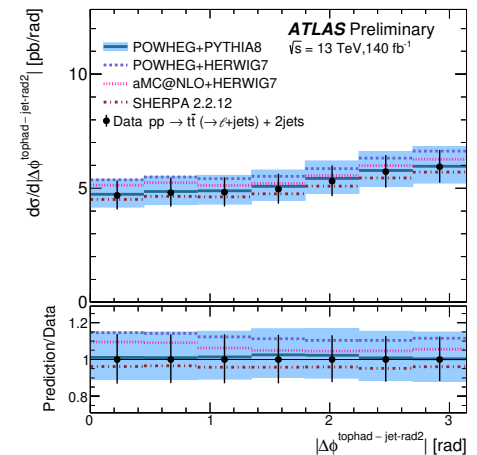
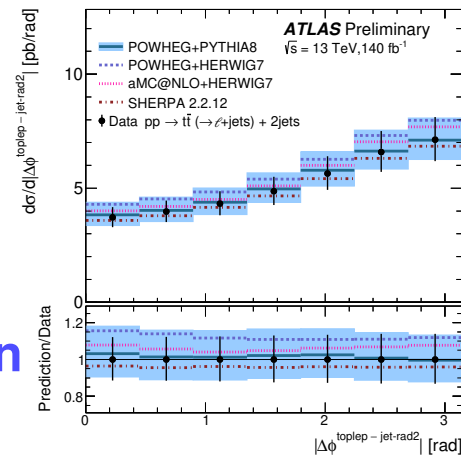


Results

- Absolute differential cross sections for $t\bar{t}+2$ jets channel vs NLO:
- **Motivation:** characterisation of kinematics, dynamics and topology of second-hardest emission

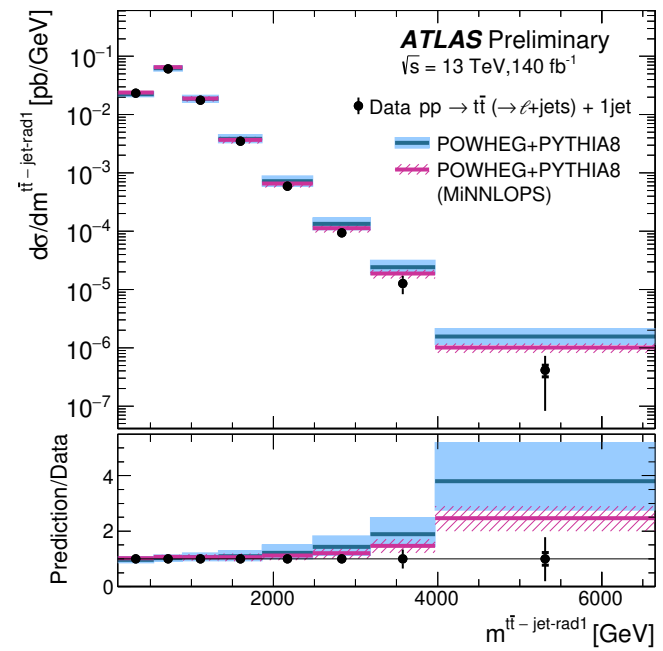
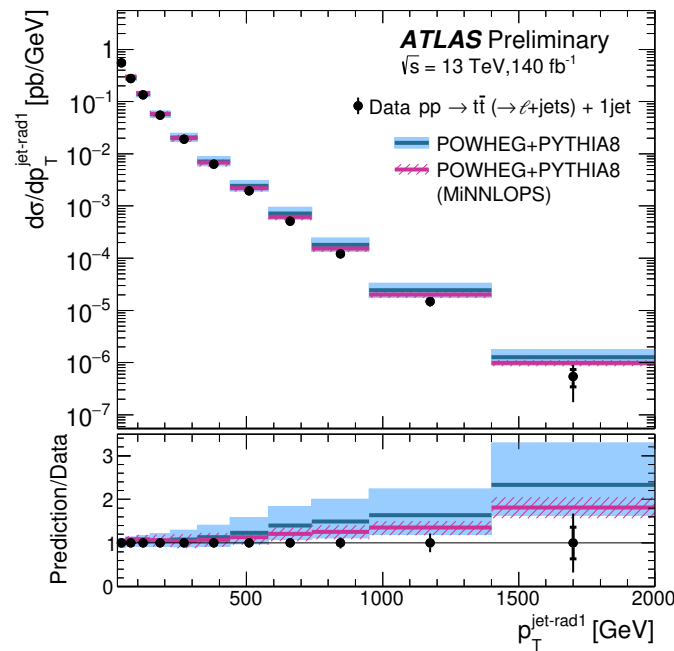
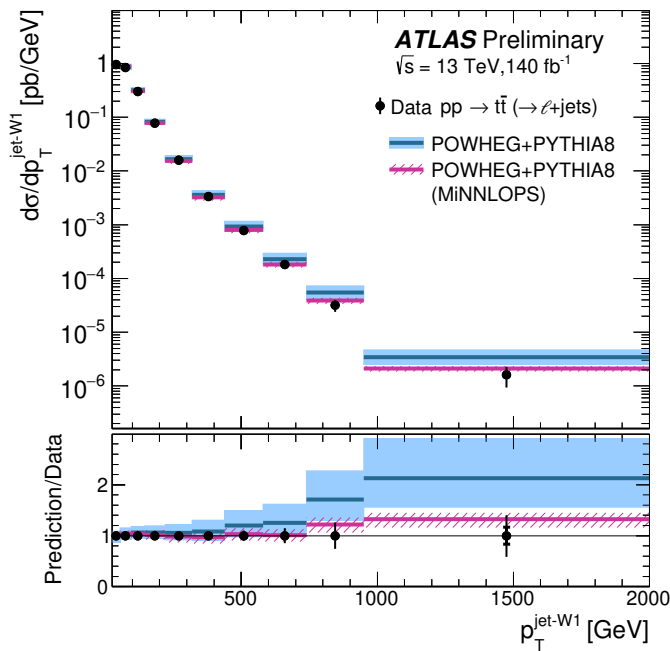
- Measured cross sections as functions of $|\Delta\phi^{\text{tolep}} - \text{jet-rad2}|$ and $|\Delta\phi^{\text{tophad}} - \text{jet-rad2}|$ have different shapes
 → the hard radiation tends to be farther in ϕ from the tolep than from the tophad and more isotropic than for first emission

- **Comparison with NLO QCD predictions:**
 - good description of angular observables
 - good description of $p_T^{\text{jet-rad2}}$ and $m^{\text{jet-rad1} - \text{jet-rad2}}$ by SHERPA and POWHEG



Results

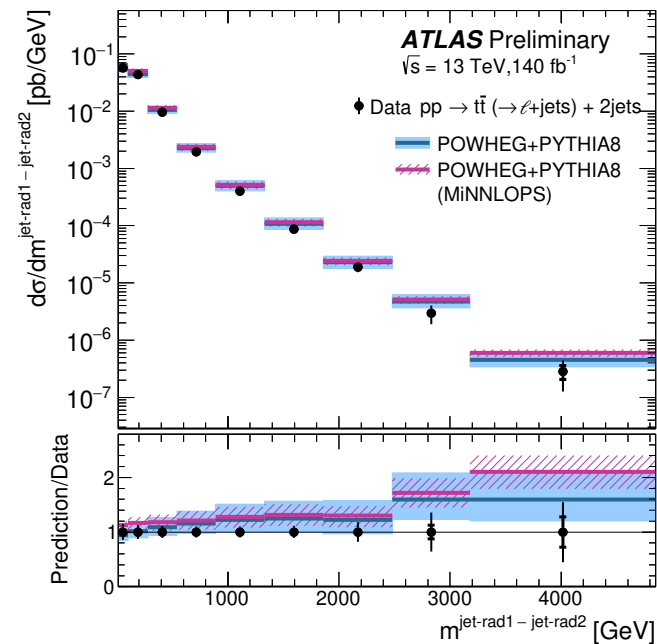
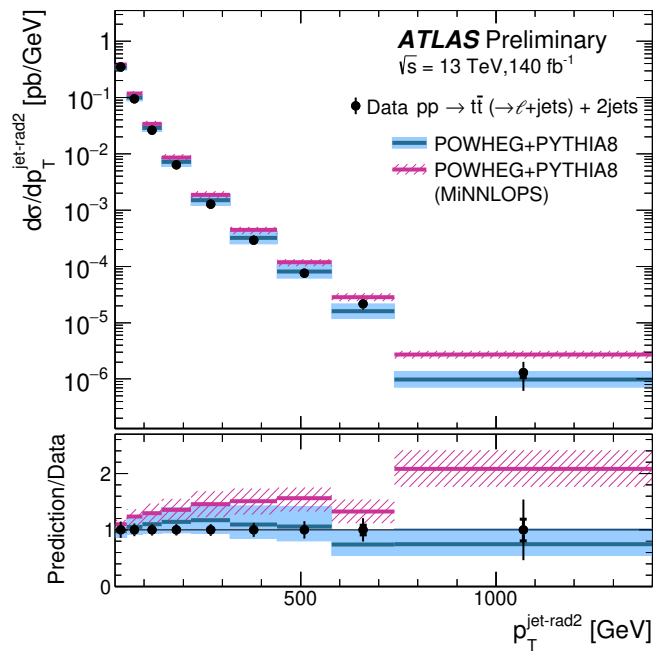
● Absolute differential cross sections vs NLO and NNLO:



⇒ Improved description of the $p_T^{\text{jet-W1}}$, $p_T^{\text{jet-rad1}}$ and $m^{\text{t}\bar{\text{t}} - \text{jet-rad1}}$ measured cross sections by the NNLO predictions from PWG+Py8 MINNLOPS

Results

● Absolute differential cross sections vs NLO and NNLO:



⇒ Description of $p_T^{\text{jet-rad2}}$ and $m^{\text{jet-rad1} - \text{jet-rad2}}$ measured cross sections by NNLO does not improve

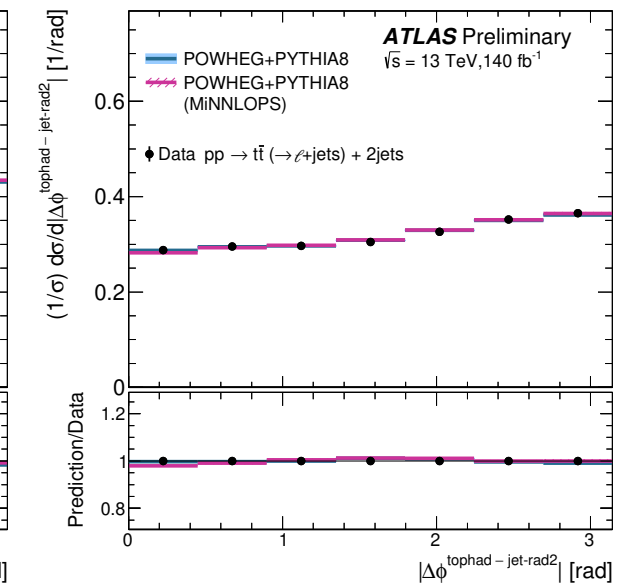
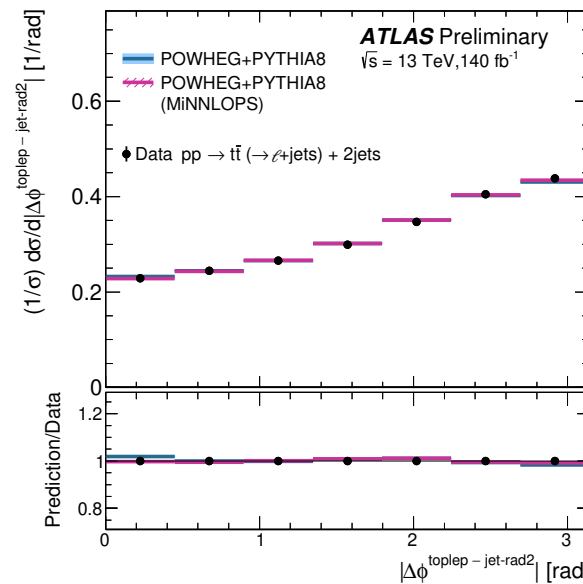
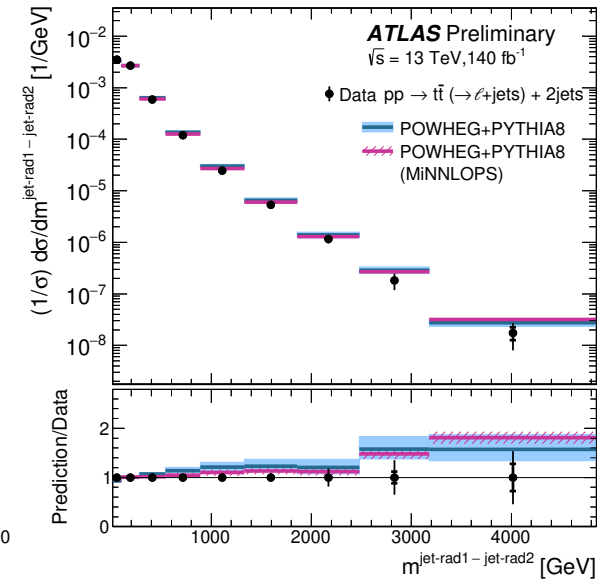
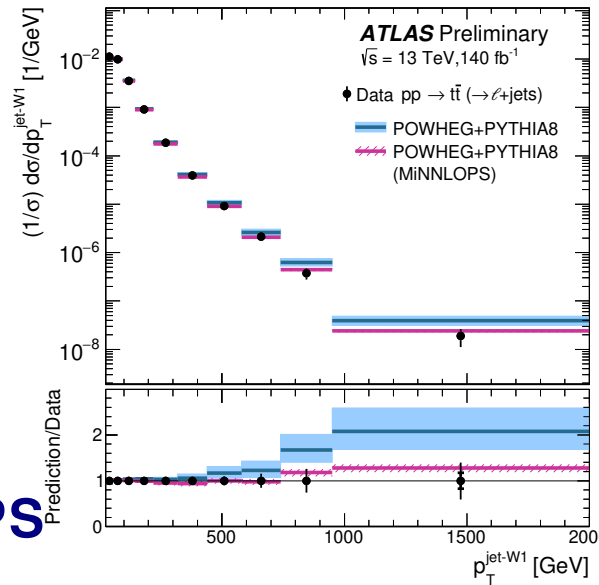
→ PWG+PY8 MNNLOPS prediction is only lowest order for second emission



Results

- Some normalised differential cross sections vs NLO and NNLO:
- ⇒ Reduction of experimental and theoretical uncertainties

⇒ Good description of measured normalised differential cross sections by PWG+PY8 MINNLOPS with reduced theoretical and experimental uncertainties

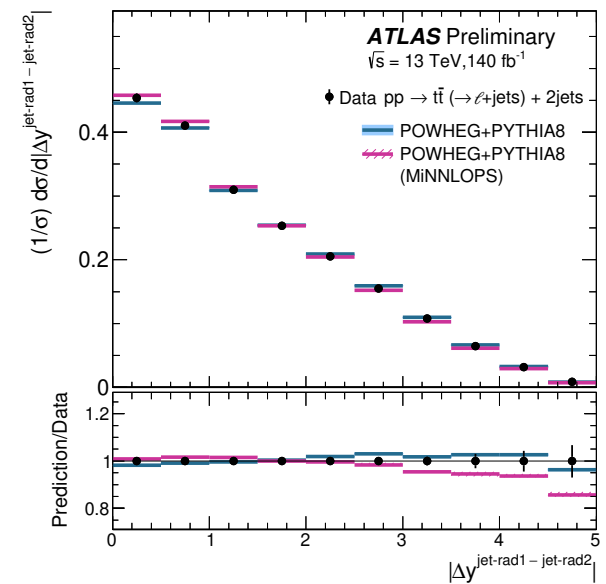
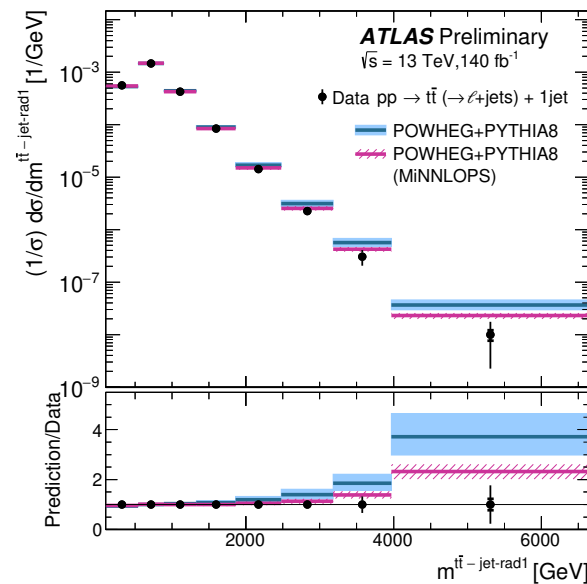
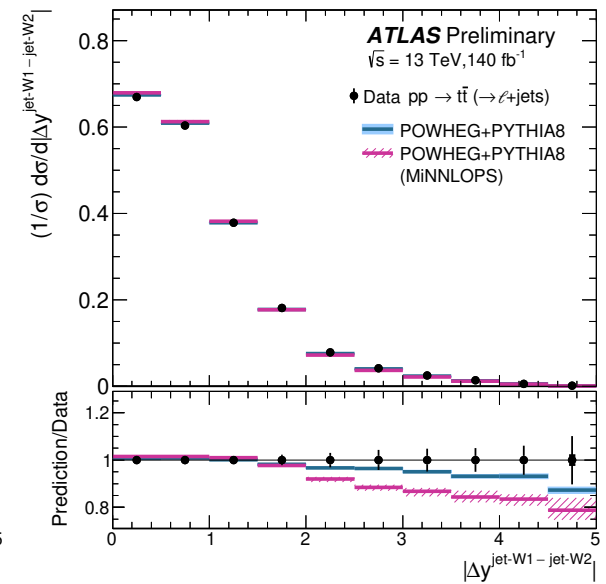
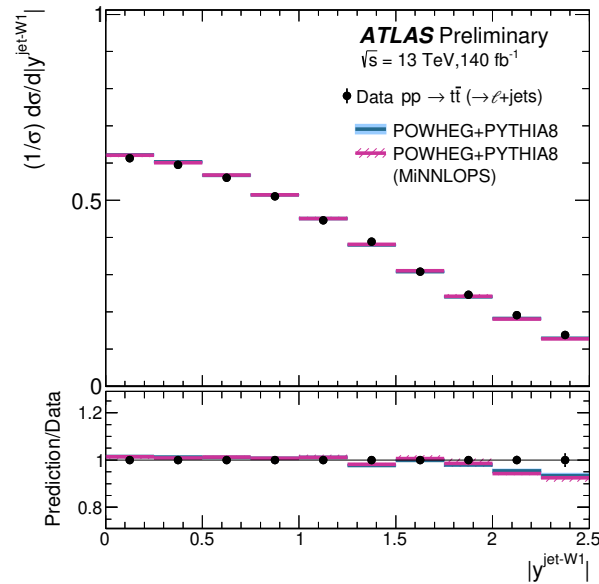




Results

- Some normalised differential cross sections vs NLO and NNLO:
- ⇒ Reduction of experimental and theoretical uncertainties

⇒ Some regions of phase space are not well described by the predictions tested with the assumptions on the correlations in the theoretical and experimental uncertainties considered



Summary and conclusions

- **Absolute and normalised differential cross sections at particle level measured for $t\bar{t}$ (+jets) production in ℓ +jets decay mode using 140 fb^{-1} of ATLAS data at $\sqrt{s} = 13 \text{ TeV}$**
- **Jet angular correlations, jet transverse momenta and invariant masses in the $t\bar{t}$ inclusive, $t\bar{t} + 1 \text{ jet}$ and $t\bar{t} + 2 \text{ jets}$ channels were measured**
- **The measurements were used to characterise the jets forming the hadronically-decaying top and the dynamics of the first and second emissions**
→ **the topology of the first and second QCD emissions were found to have different characteristics**
- **The NLO predictions describe well the shape of the angular observables, but the transverse momenta and invariant masses are described in general only by SHERPA**
- **The NNLO QCD predictions give an improved description of some of the transverse momentum and invariant mass measured cross sections with smaller theoretical uncertainties**
- **The normalised cross sections, with reduced uncertainties, show that there are regions of phase space in which the predictions tested do not describe the data with the assumptions on the correlations in the theoretical and experimental uncertainties considered and that further tuning of the PS is necessary**

Back up

Observables I

- Observables in $t\bar{t}$ inclusive ($N^{\text{jets}} \geq 4$, no additional jets explicitly requested)

→ transverse momenta of jets:

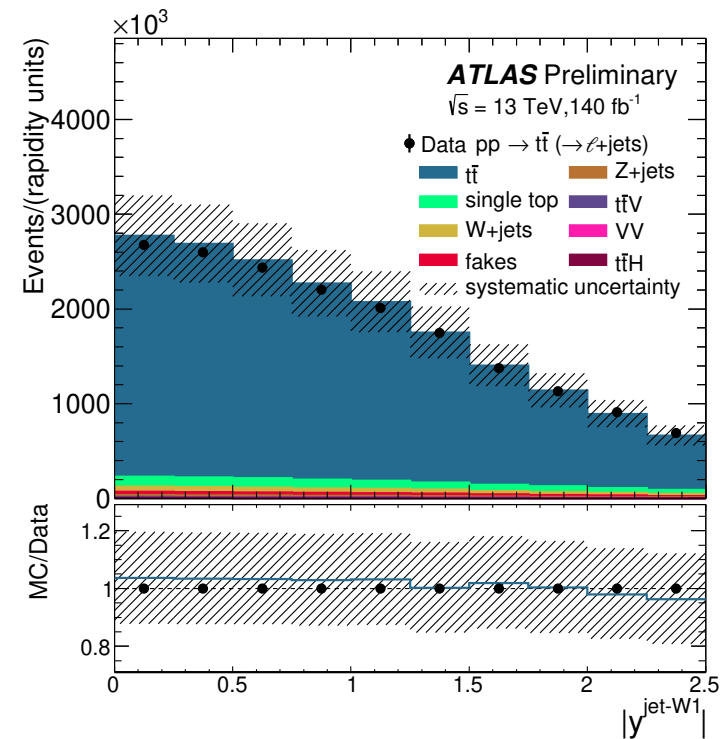
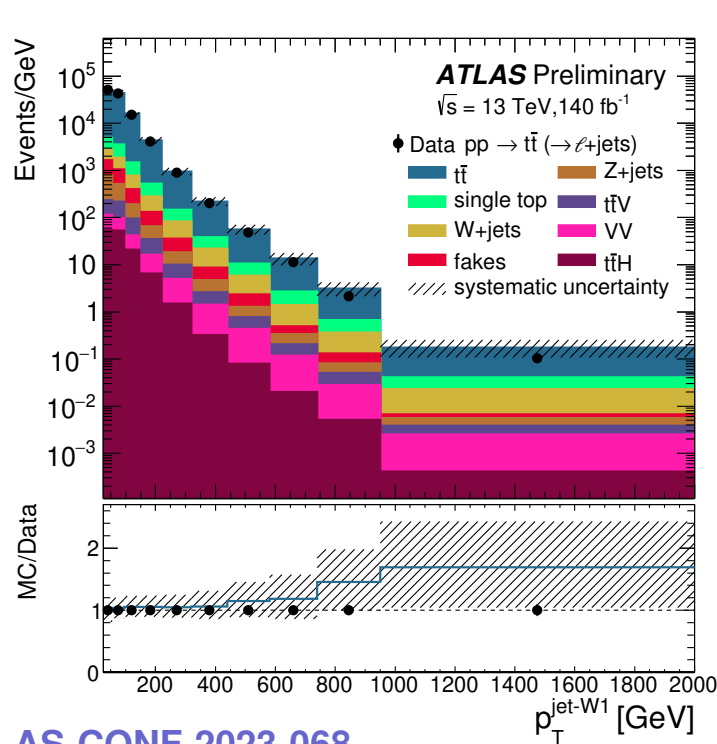
$$p_T^{\text{jet-W1}} \text{ and } p_T^{\text{jet-W2}}$$

→ angular correlations:

$$|\Delta y^{\text{jet-W1} - \text{jet-W2}}| \text{ and } |\Delta \phi^{\text{jet-W1} - \text{jet-W2}}|$$

→ rapidities of jets:

$$|y^{\text{jet-W1}}| \text{ and } |y^{\text{jet-W2}}|$$



Observables II

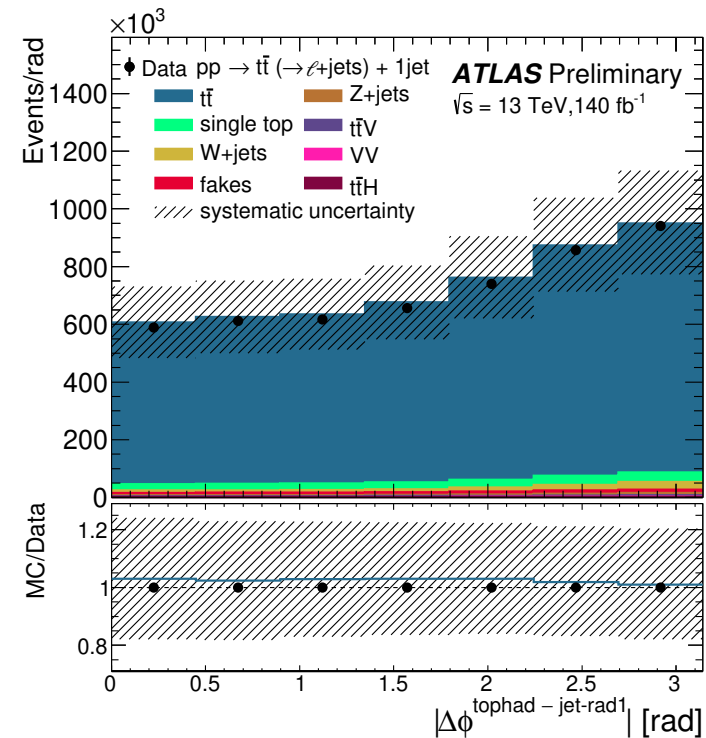
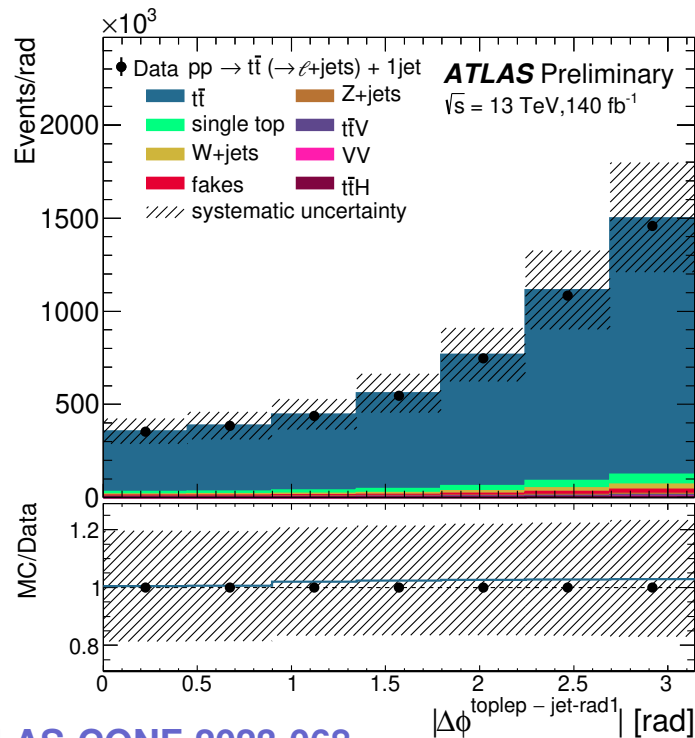
- Observables in $t\bar{t}+1$ jet ($N^{\text{jets}} \geq 5$, one additional jet explicitly requested)

→ transverse momentum and rapidity of additional jet: $p_T^{\text{jet-rad1}}$ $|y^{\text{jet-rad1}}|$

→ angular correlations:

$|\Delta\phi^{\text{jet-W1-jet-rad1}}|$, $|\Delta\phi^{\text{tolep-jet-rad1}}|$ and $|\Delta\phi^{\text{tophad-jet-rad1}}|$

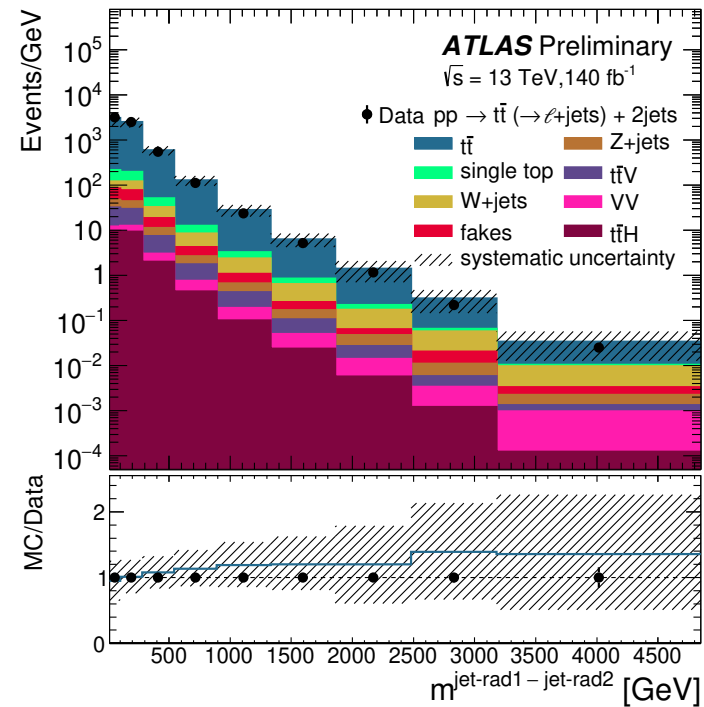
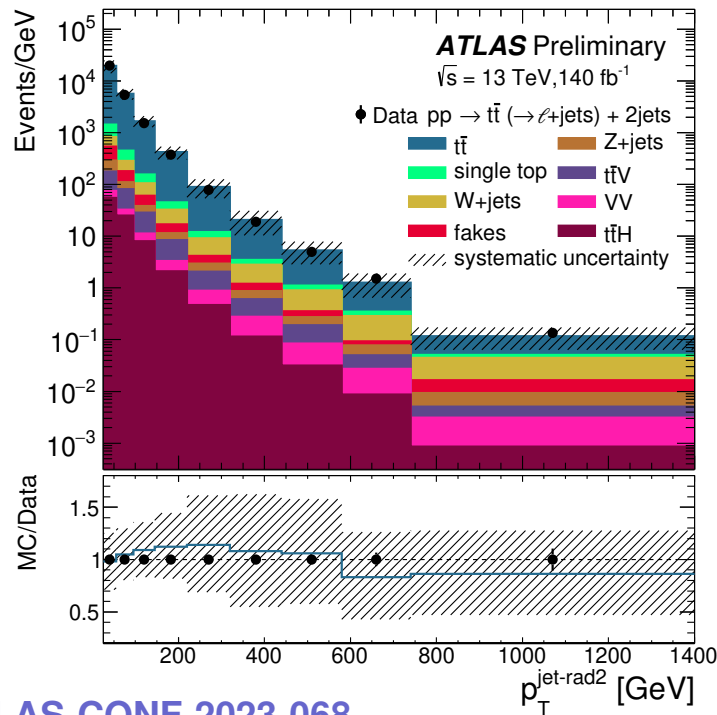
→ invariant mass: $m^{t\bar{t}-\text{jet-rad1}}$



Observables III

- Observables in $t\bar{t}+2$ jets ($N^{\text{jets}} \geq 6$, two additional jets explicitly requested)

- transverse momentum and rapidity of additional jet: $p_T^{\text{jet-rad2}}$ and $|y^{\text{jet-rad2}}|$
- angular correlations: $|\Delta y^{\text{jet-rad1} - \text{jet-rad2}}|$, $|\Delta\phi^{\text{jet-rad1} - \text{jet-rad2}}|$, $|\Delta\phi^{\text{toplep} - \text{jet-rad2}}|$, $|\Delta\phi^{\text{tophad} - \text{jet-rad2}}|$ and $|\Delta\phi^{\text{jet-W1} - \text{jet-rad2}}|$
- invariant mass: $m^{\text{jet-rad1} - \text{jet-rad2}}$



Unfolding

- The data distributions, after background subtraction, were unfolded using the iterative application of Bayes theorem with 2 iterations to obtain the measured differential cross sections at particle level using unfolding matrices with detector- and particle-level objects which are angularly well matched (to suppress combinatorial background)

$$\frac{d\sigma}{dX_i} \equiv \frac{1}{\mathcal{L} \cdot \Delta X_i} \cdot N_i^{\text{unf}}$$

$$N_i^{\text{unf}} \equiv \frac{1}{\varepsilon^i} \cdot \sum_j f_{\text{match}}^j \cdot \mathcal{M}_{ij}^{-1} \cdot f_{\text{acc}}^j \cdot (N_{\text{detector}}^j - N_{\text{bkg}}^j)$$

$$f_{\text{acc}}^j = \frac{N_{\text{particle} \wedge \text{detector}}^j}{N_{\text{detector}}^j}$$

$$f_{\text{match}}^j = \frac{N_{\text{particle} \wedge \text{detector} \wedge \text{match}}^j}{N_{\text{particle} \wedge \text{detector}}^j}$$

$$\varepsilon^i = \frac{N_{\text{particle} \wedge \text{detector}}^i}{N_{\text{particle}}^i}$$

